

## Research Article

# Cardiorespiratory Frequency Monitoring Using the Principal Component Analysis Technique on UWB Radar Signal

**Erika Pittella, Anna Bottiglieri, Stefano Pisa, and Marta Cavagnaro**

*Department of Information Engineering, Electronics and Telecommunications, Sapienza University of Rome, Rome, Italy*

Correspondence should be addressed to Erika Pittella; [pittella@diet.uniroma1.it](mailto:pittella@diet.uniroma1.it)

Received 4 September 2016; Revised 6 January 2017; Accepted 12 February 2017; Published 2 March 2017

Academic Editor: Symeon Nikolaou

Copyright © 2017 Erika Pittella et al. This is an open access article distributed under the Creative Commons Attribution License, which permits unrestricted use, distribution, and reproduction in any medium, provided the original work is properly cited.

In this paper, Principal Component Analysis technique is applied on the signal measured by an ultra wide-band radar to compute the breath and heart rate of volunteers. The measurement set-up is based on an indirect time domain reflectometry technique, using an ultra wide-band antenna in contact with the subject's thorax, at the heart height, and a vector network analyzer. The Principal Component Analysis is applied on the signal reflected by the thorax and the obtained breath frequencies are compared against measures acquired by a piezoelectric belt, a widely used commercial system for respiratory activity monitoring. Breath frequency results show that the proposed approach is suitable for breath activity monitoring. Moreover, the wearable ultra wide-band radar gives also promising results for heart activity frequency detection.

## 1. Introduction

Continuous monitoring of breath rate is one of the most important issues to detect patients' respiratory diseases throughout hospitalization time and home therapy periods. Usually, breath monitoring is performed using a piezoelectric belt, wrapped around the patient body. However, this equipment can be uncomfortable or can give rise to artifacts [1].

Heart activity is conventionally measured through electrocardiography apparatuses using on-body electrodes [2] or using the pulse oximetry [3]. This latter device has been realized for the monitoring of oxygen saturation in blood but it gives information on the heart rate also. Both systems are reliable and provide good signal quality; however, they are problematic and inadequate for long-term, everyday measurements. Moreover, these devices require direct contact of the sensor with the body.

A possible alternative solution for the heart and breath activity monitoring is the use of ultra wide-band (UWB) radars. The working principle is the typical one of radars: an impulse signal, transmitted by an antenna, is reflected by the subject thorax back to the transmitting antenna (or to a different one). If the patient's thorax moves due to breathing,

the system is able to detect the movement from the variation of the time of arrival to the antenna of the pulsed signal [4–6].

The first radar system applied for the monitoring of respiratory activity was the Doppler radar, which uses a continuous wave signal in the microwave range [7–9]. The UWB radar is a valuable alternative due to its better performances compared with the Doppler one. In fact, the use of very short pulses (of the order of hundreds of picoseconds) results in a lower interference with other systems, lower cost, and lower power density [10–12]. Moreover, the low power density radiated by the radar system allows better satisfying regulation limits settled by safety guidelines [13]. In particular, in [11] the power absorbed by the human body exposed to the field emitted by a typical UWB radar was studied and it was shown that safety aspects and regulation limits are largely satisfied.

With reference to the cardiorespiratory activity monitoring, both far-field radars and body-worn radars can be used. Typically, body-worn UWB radars are monostatic radars in which the same antenna is used to radiate the UWB signal and to receive its reflection from the human body. The UWB antenna is placed close to the thorax, so that reflections due to antenna mismatches, garments, and the first body layers, as

the skin, are substantially superimposed on the transmitted signal [14–16].

Usually, signal analysis techniques are applied to UWB radar signals placed far from the human body, to evaluate breath and heart rate removing the static clutter coming from the environment [5, 17, 18]. In [19], for the first time, signal processing techniques were used to evaluate the breath frequency of volunteers starting from signals measured by a wearable UWB radar. It is worth noting that, in the body-worn case, the static clutter is not due to the contribution of the surrounding environment, but it is due to the layers of the human body, which move together with the UWB antenna. Radar measured breath frequency was in good agreement with measurements acquired by a piezoelectric belt.

In this paper, a body-worn UWB radar system is considered. The signal reflected by the human thorax is studied in order to find breath and heart frequency of the subject under investigation. In particular, the Principal Component Analysis (PCA) technique is applied to the UWB reflected signals. The PCA technique is employed on the signal obtained by a body-worn radar to evaluate the breath frequency of a subject. PCA is a procedure that converts a set of measurements of correlated variables into a set, with lower dimension, of linearly uncorrelated variables, called principal components. In this way the variability of the data is enhanced and the redundancy among the same data is reduced [20]. Output of the PCA analysis is the “principal component matrix,” in which every column is arranged in order of descendent variability. For this reason, in the present application the target information is included among the first columns of the principal components matrix (largest variance), while the successive columns contain the redundant information linked to the static clutter.

Measurements were performed on five subjects, with the UWB antenna [21] placed in contact with the volunteer clothes, in correspondence of the heart.

Two breath conditions were considered: normal breath and deep breath. Moreover, in one case measurements were taken while the volunteer was moving own legs and arms. For comparison purposes, during the measurement, a piezoelectric belt was used in order to acquire, in a conventional way, the breath signal. Once obtained the breath signal, the PCA technique was used to look for the heart rate of the volunteer.

The remainder of this paper is organized as follows. In Section 2, the measurement set-up and the PCA technique are described; in Section 3 results are presented and discussed. Finally, in Section 4 conclusions are drawn.

## 2. Methods and Models

*2.1. Measurement Set-Up.* Figure 1 shows a volunteer with the piezoelectric belt and the UWB antenna positioned on the thorax at the height of the heart. The piezoelectric belt (UFI model I132 Pneumotrace II™) is constituted by a solid-state transducer, fixed on an elastic belt, and it is used to measure changes in chest or abdominal circumference linked to the respiratory activity.

The transducer transforms the mechanical movement into electric voltage, generating a positive voltage as the belt



FIGURE 1: The piezoelectric belt and the UWB radar antenna.

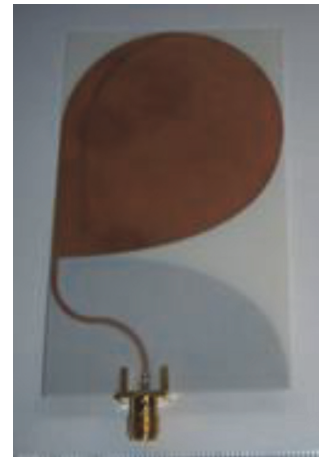


FIGURE 2: UWB antenna used in the radar.

length increases. Its typical output signal, during normal breathing, has a dynamics of about 50 mV.

The body-worn UWB radar was realized through an indirect time domain reflectometry (TDR) technique [16]. The TDR technique measures the frequency spectrum of the antenna reflection coefficient, multiplies it by the spectrum of a monocycle pulse, and transforms the obtained signal in the time domain through an Inverse Fast Fourier Transform (IFFT). In this way, the reflected echo time behaviour is evaluated. In particular, in the used set-up a vector network analyzer (Agilent PNA E8363C) measured the antenna reflection coefficient in the 10 MHz–10 GHz frequency band, with a sampling frequency of 10 MHz (i.e., 1000 frequency points). Several acquisitions were performed in sequence to sample the respiratory activity. To this end, a dedicated VBA macro was used in order to increase the acquisition speed. The macro allows recording three-hundred reflection coefficient traces during an experimental session of about 30 s; then it stores the traces in the PNA memory.

The UWB antenna utilized for the measurement is a heart-shaped UWB antenna previously designed and manufactured [22] (see Figure 2). Such an antenna was chosen

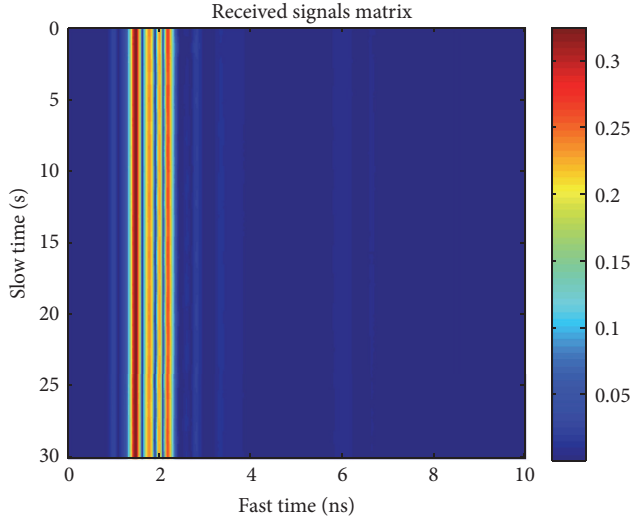


FIGURE 3: Matrix of the received signals.

because of the broadband and good radiation properties of the printed heart monopole antenna [23]. In particular, for miniaturization purposes, a microstrip-fed antipodal structure was considered, where the radiating element and the feeding microstrip line are realized over one of the substrate faces, while on the other face a suitable ground plane is etched [21, 23, 24].

After the measurement session, the reflected echoes were reconstructed according the steps above described, using a purposely developed LabVIEW virtual instrument (VI). The VI multiplies the spectrum of each measured reflection coefficient by the spectrum of a monocycle pulse 100 ps wide; then it transforms the obtained waveforms back in the time domain, thus obtaining 300 different waveforms, to be used in the successive postprocessing signal analysis. Each waveform lasts 100 ns and it is sampled with a time-step of 10 ps (10001 time points).

The reconstructed signals were arranged in a  $N_w = 300 \times N_s = 10001$  matrix. The column index, referring to the sampling times, is defined as the “fast-time,” and the row index, indicating the different received waveforms, is named the “slow-time.” Figure 3 shows an example of the obtained matrix, where colours are used to represent different signal strengths. Since the information linked to the breath and heart activity is located around 7 ns [11, 15], only the first 10 ns of the reflected signals is shown in the figure.

As can be noted from Figure 3, the received waveforms show high values at short fast-time (red colours), which means that strong reflections are recorded by the antenna as soon as the incident pulse is radiated. These reflections are partly due to antenna mismatches and partly come from the first layers of the subject (garments and skin). They slightly change (straight vertical lines in Figure 3) with the respiration because the antenna, fixed to the body, moves synchronously with the thorax. Therefore, these strong reflections represent the static clutter, which covers the useful signal and has to be removed.

**2.2. Principal Component Analysis.** To eliminate the static echo present in the received waveforms, the PCA method was used.

The PCA technique highlights the variability of a signal and restrains its redundancy. The starting point of the PCA algorithm is the matrix of the received signals,  $R$ , which has dimensions  $N_w \times N_s$ . As a preliminary step, the mean value of the samples is calculated on each row of  $R$ , that is, on each waveform, and subtracted from every measure. The result of this operation is a zero-mean matrix, here below named  $\hat{R}$ , in which a first correlation among the samples, for each observation, was eliminated.

Starting from  $\hat{R}$ , the purpose of PCA is to find a new matrix  $Y$  that will be the matrix of principal components, given by

$$Y = \hat{R}T, \quad (1)$$

where  $T$  is the matrix that transforms  $\hat{R}$  into  $Y$ . As shown here below,  $T$  can be computed using the covariance matrix  $S_R$  of the  $\hat{R}$  matrix:

$$S_R = \frac{1}{N_w - 1} \hat{R}^T \hat{R}. \quad (2)$$

$S_R$  is a symmetric matrix, whose eigenvalues are arranged on the principal diagonal of the matrix  $\Lambda$  in descendent order, and the eigenvectors constitute the columns of the  $U$  matrix.

In particular,  $U$  and  $\Lambda$  satisfy the following equation:

$$S_R = U\Lambda U^T. \quad (3)$$

The  $T$  matrix in (1) is chosen equal to the  $U$  matrix. The reason of this choice can be understood evaluating the covariance matrix  $S_y$  of  $Y$ , given by

$$\begin{aligned} S_y &= \frac{1}{N_w - 1} Y^T Y = \frac{1}{N_w - 1} (\hat{R}T)^T \hat{R}T \\ &= T^T \left( \frac{1}{N_w - 1} (\hat{R}^T \hat{R}) \right) T = T^T S_R T. \end{aligned} \quad (4)$$

The purpose is to obtain a matrix  $Y$  such that the covariance matrix  $S_y$  has the largest variance, which is linked to the variability of the data, and the minimum covariance, which is linked to the redundancy of the data. It is required that  $S_y$  is a diagonal matrix, as shown in

$$\begin{aligned} S_y &= T^T S_R T = \begin{bmatrix} t_1^T \\ t_2^T \\ \vdots \\ t_{N_s}^T \end{bmatrix} [S_{R_1} \ \cdots \ S_{R_2}] [t_1 \ t_2 \ \cdots \ t_{N_s}] \\ &= \begin{bmatrix} \lambda_1 & \cdots & 0 \\ \vdots & \ddots & \vdots \\ 0 & \cdots & \lambda_{N_s} \end{bmatrix}. \end{aligned} \quad (5)$$

This result is achieved with  $T$  equal to  $U$  and  $S_R$  as in (3).

Once the  $T$  matrix is evaluated, the  $Y$  matrix can be calculated according to (1). Through the  $Y$  matrix a rotation from the original matrix to a new one is performed. In the new matrix the redundant components, represented by the static clutter, are moved to columns with higher index. Accordingly, in the columns of  $Y$  with the highest absolute value, the respiratory signal should be present.

In this paper, once the static clutter was removed through the PCA technique, the FFT was performed in the slow-time looking for periodical behaviours. In particular, since it was observed that the echo from the lungs appeared at about 7 ns from the first reflection [15, 16], the FFT was performed on the columns of the matrix representing time instants from 1 ns to 10 ns and the column with the highest spectral component was considered the one reporting the respiratory signal.

Noting that the cardiac signal is superimposed to the respiratory signal [19], it is possible to look for the cardiac frequency also. To this end, the first harmonics of the respiratory signal that have frequencies between 0.2 Hz and 0.8 Hz should be removed first, because they are sufficiently strong to hide the feeble cardiac signal that has frequencies in a close frequency range (between 0.8 Hz and 3 Hz). For this reason a particular filter, called *comb* filter [4], can be used, which removes the breath frequency and its subsequent harmonics. Afterwards, a specific high-pass filter can be used in order to isolate the cardiac frequency.

### 3. Results

**3.1. Breath Activity.** Five different subjects were considered, two males and three females. Measurements were taken during normal breath and deep breath and, in one case, while a volunteer moved arms and legs. A total of 12 measures were considered.

Elaboration was performed applying the previously described PCA technique to filter out the static components in the received signal. As an example, Figure 4 shows the PCA filtered matrix obtained from the data in Figure 3. Then, the FFT was applied on the columns of the filtered matrix and the highest spectral component was taken as the breath frequency. Figure 5 shows the time behaviour of the column of the PCA filtered matrix (Figure 4) where the highest spectral component was obtained. As can be observed from the figure, the obtained time behaviour has an approximately sinusoidal form, representing the breathing activity. However, signal components of higher frequencies are superimposed over the simple sinusoid. This can be explained by the presence of the heart signal, which is superimposed to the breath one, as well as by the presence of some noise not completely cancelled out by the filtering technique.

Table 1 shows the breath frequency obtained by the PCA for five volunteers (ID1 to ID5), in different measurement conditions.

In the table, the breath frequency obtained by the UWB radar through the PCA analysis is compared with the frequency measured by the piezoelectric belt. In the table the

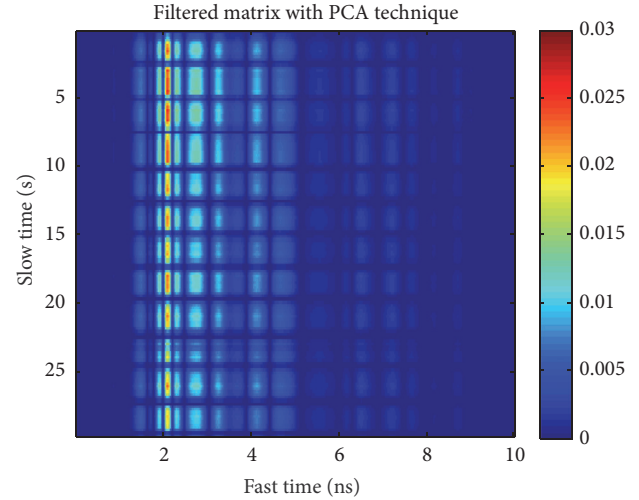


FIGURE 4: Received signal matrix after the application of the PCA technique.

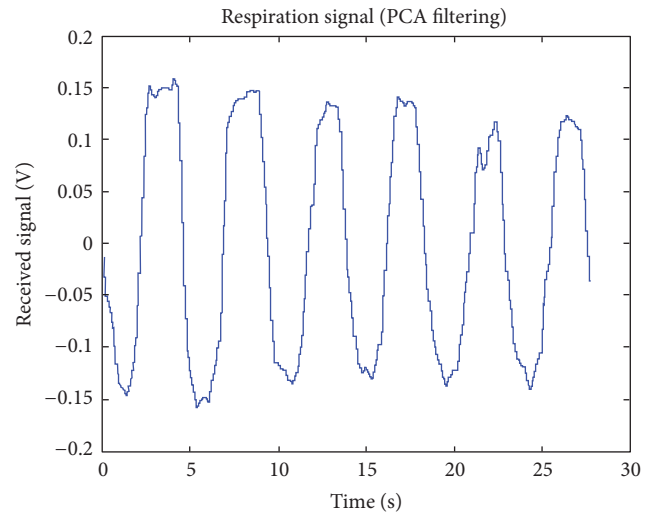


FIGURE 5: Time behaviour of the column with the highest spectral component obtained after evaluating the FFT on the matrix filtered by PCA.

time needed by the PCA method to elaborate the breath data ( $t_e$ ) is also shown.

As can be noted from the table, in all cases the normal breath shows a frequency slightly higher than the deep breath, as expected, because when the breath is deeper the thorax movement is long-lasting and its frequency lowers.

When the subject moves the arms (#4), since this movement changes the piezoelectric belt length, with a greater extent than the respiratory activity, an error is induced in the belt data as clearly visible in row number 4 of Table 1. On the other hand, it is very interesting to note that while the belt fails, being the belt signal completely masked by the subjects' movements, the PCA computes a frequency a little bit higher than the frequency evaluated in the normal respiration condition, as expectable.

TABLE 1: Breath frequency measurement results.

#	People	Meas. condition	Belt $f$ (Hz)	PCA, breath $f$ (Hz)	$t_e$ (s)
1	ID 1	Deep	0.22	0.22	2.33
2		Deep	0.22	0.22	2.26
3		Normal	0.26	0.26	2.25
4		Moving	0.03	0.37	2.24
5	ID 2	Deep	0.26	0.26	2.31
6		Normal	0.39	0.37	2.53
7	ID 3	Deep	0.26	0.26	2.22
8		Normal	0.30	0.29	2.23
9	ID 4	Deep	0.27	0.26	2.28
10		Normal	0.31	0.29	2.26
11	ID 5	Deep	0.22	0.22	2.26
12		Normal	0.37	0.15	2.24

TABLE 2: Heart frequency measurement results.

#	People	Meas. condition	PCA, heart $f$ (Hz)
1	ID 1	Deep	1.19
2		Deep	1.19
3		Normal	1.23
4		Moving	1.38
5	ID 2	Deep	1.24
6		Normal	1.38
7	ID 3	Deep	1.22
8		Normal	1.25
9	ID 4	Deep	1.26
10		Normal	0.99
11	ID 5	Deep	1.19
12		Normal	1.00

Taking into account the belt results as a reference, with the exception of measure #4 (i.e., moving case, because of belt failure) and #12 (where the PCA shows a breath frequency value considerably different from that obtained by the belt), the PCA technique has a maximum relative error  $e_r$  lower than 5% in all measures.

**3.2. Preliminary Results on Heart Activity.** In Table 2 the cardiac frequency results obtained by means of the wearable UWB radar system are shown. Results achieved with the UWB radar are close to the standard values of the cardiac frequency ( $\approx 1$  Hz).

Figure 6 shows the voltage spectrum of the cardiac signal computed by the PCA technique. These results on the heart rate are encouraging and suggest deepening the analysis for demonstrating the feasibility of heart activity monitoring by wearable UWB radar systems.

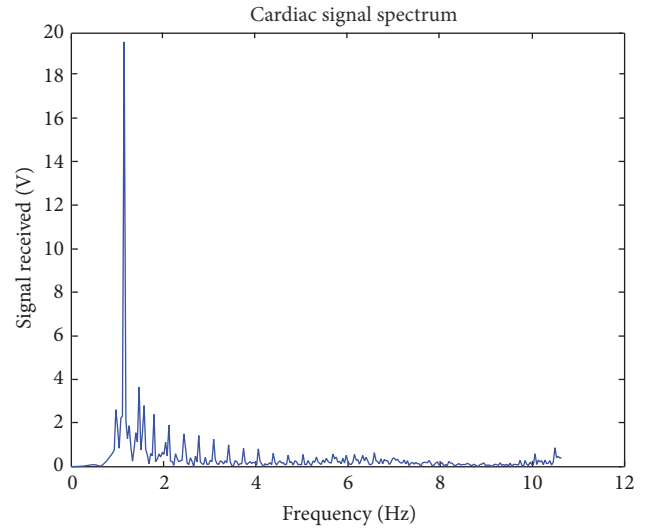


FIGURE 6: Spectrum of the cardiac signal.

## 4. Conclusions

In this paper the monitoring of the cardiorespiratory activity by a wearable UWB radar is addressed. The PCA method is used as signal elaboration technique to deal with the problem. Obtained results of the respiratory frequency are comparable with a traditional technique (i.e., the piezoelectric belt) for normal and deep respiratory condition. Moreover, in the cases where the piezoelectric belt fails, that is, in the case of normal breath with movement of the arms, the UWB radar shows results in compliance with standard values.

Concerning the heart activity, UWB radar results are encouraging. As future work, an additional campaign of measurements that will involve a wider number of volunteers of different sex and age will be performed, in order to test the validity of the proposed method for finding the heart rate. Moreover, for comparison purposes, in order to confirm the results, a conventional measuring technique of the heart rate as, for example, a pulse oximeter, will be used also.

## Competing Interests

The authors declare that there is no conflict of interests regarding the publication of this paper.

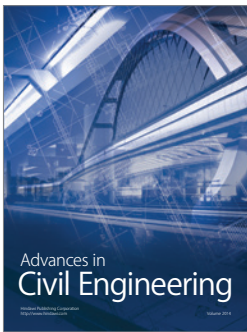
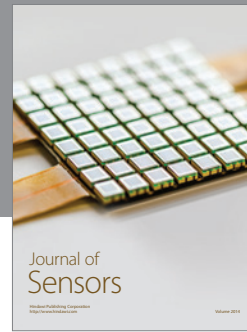
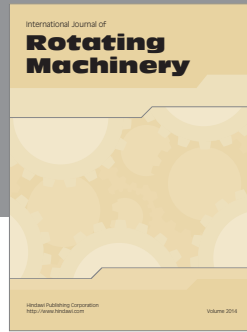
## Acknowledgments

The authors would like to acknowledge Dr. Cristina Raja (Keysight Technologies) for her support in the VBA macro implementation.

## References

- [1] R. Marani, G. Gelao, and A. G. Perri, "A new system for continuous monitoring of breathing and kinetic activity," *Journal of Sensors*, vol. 2010, Article ID 434863, 6 pages, 2010.
- [2] N. Meziane, J. G. Webster, M. Attari, and A. J. Nimunkar, "Dry electrodes for electrocardiography," *Physiological Measurement*, vol. 34, no. 9, pp. R47–R69, 2013.

- [3] P. A. Kyriacou, M. Hickey, and J. P. Phillips, "Pulse oximetry of body cavities and organs," in *Proceedings of the 35th Annual International Conference of the IEEE Engineering in Medicine and Biology Society (EMBC '13)*, pp. 2664–2667, Osaka, Japan, July 2013.
- [4] A. Lazaro, D. Girbau, and R. Villarino, "Analysis of vital signs monitoring using an IR-UWB radar," *Progress in Electromagnetics Research*, vol. 100, pp. 265–284, 2010.
- [5] S. Venkatesh, C. Anderson, N. V. Rivera, and R. M. Buehrer, "Implementation and analysis of respiration-rate estimation using impulse-based UWB," in *Proceedings of the IEEE Military Communications Conference (MILCOM '05)*, vol. 5, pp. 3314–3320, Atlantic City, NJ, USA, October 2005.
- [6] P. Bernardi, R. Cicchetti, S. Pisa, E. Pittella, E. Piuze, and O. Testa, "Design, realization, and test of a UWB radar sensor for breath activity monitoring," *IEEE Sensors Journal*, vol. 14, no. 2, pp. 584–596, 2014.
- [7] A. D. Droitcour, O. Boric-Lubecke, V. M. Lubecke, J. Lin, and G. T. A. Kovacs, "Range correlation and I/Q performance benefits in single-chip silicon Doppler radars for noncontact cardiopulmonary monitoring," *IEEE Transactions on Microwave Theory and Techniques*, vol. 52, no. 3, pp. 838–848, 2004.
- [8] F. Soldovieri, I. Catapano, L. Crocco, L. N. Anishchenko, and S. I. Ivashov, "A feasibility study for life signs monitoring via a continuous-wave radar," *International Journal of Antennas and Propagation*, vol. 2012, Article ID 420178, 5 pages, 2012.
- [9] L. Scalise, V. Mariani Primiani, P. Russo, A. De Leo, D. Shahu, and G. Cerri, "Wireless sensing for the respiratory activity of human beings: measurements and wide-band numerical analysis," *International Journal of Antennas and Propagation*, vol. 2013, Article ID 396459, 10 pages, 2013.
- [10] J. C. Y. Lai, Y. Xu, E. Gunawan et al., "Wireless sensing of human respiratory parameters by low-power ultrawideband impulse radio radar," *IEEE Transactions on Instrumentation and Measurement*, vol. 60, no. 3, pp. 928–938, 2011.
- [11] M. Cavagnaro, E. Pittella, and S. Pisa, "Evaluation of the electromagnetic power absorption in humans exposed to plane waves: the effect of breathing activity," *International Journal of Antennas and Propagation*, vol. 2013, Article ID 854901, 7 pages, 2013.
- [12] Y. Yu, J. Yang, T. McKelvey, and B. Stoew, "A compact UWB indoor and through-wall radar with precise ranging and tracking," *International Journal of Antennas and Propagation*, vol. 2012, Article ID 678590, 11 pages, 2012.
- [13] ICNIRP, "Guidelines for limiting exposure to time-varying electric, magnetic, and electromagnetic fields (up to 300 GHz)," *Health Physics*, vol. 74, no. 4, pp. 494–522, 1998.
- [14] G. Varotto and E. M. Staderini, "On the UWB medical radars working principles," *International Journal of Ultra Wideband Communications and Systems*, vol. 2, no. 2, pp. 83–93, 2011.
- [15] M. Cavagnaro, E. Pittella, and S. Pisa, "UWB pulse propagation into human tissues," *Physics in Medicine and Biology*, vol. 58, no. 24, pp. 8689–8707, 2013.
- [16] E. Pittella, S. Pisa, and M. Cavagnaro, "Breath activity monitoring with wearable UWB radars: measurement and analysis of the pulses reflected by the human body," *IEEE Transactions on Biomedical Engineering*, vol. 63, no. 7, pp. 1447–1454, 2016.
- [17] A. Nezirović, A. G. Yarovoy, and L. P. Ligthart, "Signal processing for improved detection of trapped victims using UWB radar," *IEEE Transactions on Geoscience and Remote Sensing*, vol. 48, no. 4, pp. 2005–2014, 2010.
- [18] A. Lazaro, D. Girbau, and R. Villarino, "Techniques for clutter suppression in the presence of body movements during the detection of respiratory activity through UWB radars," *Sensors*, vol. 14, no. 2, pp. 2595–2618, 2014.
- [19] E. Pittella, B. Zanaj, S. Pisa, and M. Cavagnaro, "Measurement of breath frequency by body-worn UWB radars: a comparison among different signal processing techniques," *IEEE Sensors Journal*, vol. 17, no. 6, pp. 1772–1780, 2017.
- [20] P. K. Verma, A. N. Gaikwad, D. Singh, and M. J. Nigam, "Analysis of clutter reduction techniques for through wall imaging in UWB range," *Progress In Electromagnetics Research B*, no. 17, pp. 29–48, 2009.
- [21] E. Pittella, P. Bernardi, M. Cavagnaro, S. Pisa, and E. Piuze, "Design of UWB antennas to monitor cardiac activity," *Applied Computational Electromagnetics Society Journal*, vol. 26, no. 4, pp. 267–274, 2011.
- [22] W.-S. Chen and S.-C. Wu, "A printed heart monopole antenna with band-rejected characteristics for IEEE 802.16A and UWB applications," *Microwave Journal*, vol. 50, no. 5, pp. 164–176, 2007.
- [23] E. Gazit, "Improved design of the vivaldi antenna," *IEEE Proceedings H: Microwaves, Antennas and Propagation*, vol. 135, no. 2, pp. 89–92, 1988.
- [24] K. S. Yngvesson, T. L. Korzeniowski, Y.-S. Kim, E. L. Kollberg, and J. F. Johansson, "The tapered slot antenna—a new integrated element for millimeter-wave applications," *IEEE Transactions on Microwave Theory and Techniques*, vol. 37, no. 2, pp. 365–374, 1989.



**Hindawi**

Submit your manuscripts at  
<https://www.hindawi.com>

